

Piracy Resistant Watermarks for Deep Neural Networks

Huiying Li, Emily Wenger, Shawn Shan, Ben Y. Zhao, Haitao Zheng
Department of Computer Science, University of Chicago
{huiyingli, ewillson, shansixiong, ravenben, htzheng}@cs.uchicago.edu

Abstract

As companies continue to invest heavily in larger, more accurate and more robust deep learning models, they are exploring approaches to monetize their models while protecting their intellectual property. Model licensing is promising, but requires a robust tool for owners to claim ownership of models, *i.e.* a watermark. Unfortunately, current designs have not been able to address *piracy attacks*, where third parties falsely claim model ownership by embedding their own “pirate watermarks” into an already-watermarked model.

We observe that resistance to piracy attacks is fundamentally at odds with the current use of incremental training to embed watermarks into models. In this work, we propose *null embedding*, a new way to build piracy-resistant watermarks into DNNs that can only take place at a model’s initial training. A null embedding takes a bit string (watermark value) as input, and builds strong dependencies between the model’s normal classification accuracy and the watermark. As a result, attackers cannot remove an embedded watermark via tuning or incremental training, and cannot add new pirate watermarks to already watermarked models. We empirically show that our proposed watermarks achieve piracy resistance and other watermark properties, over a wide range of tasks and models. Finally, we explore a number of adaptive counter-measures, and show our watermark remains robust against a variety of model modifications, including model fine-tuning, compression, and existing methods to detect/remove backdoors. Our watermarked models are also amenable to transfer learning without losing its watermark properties.

1 Introduction

State-of-the-art deep neural networks (DNNs) today are incredibly expensive to train. For example, a new conversational model from Google Brain includes 2.6 billion parameters, and takes 30 days to train on 2048 TPU cores [2]. Even “smaller” models like ImageNet require significant training (128 GPUs for 52 hours) to add robustness properties.

As training costs continue to grow with each generation of models, providers must explore approaches to monetize models and recoup their training costs, either through Machine Learning as a Service (MLaaS) platforms (*e.g.* [23,40]) that host models, or fee-based licensing of pretrained mod-

els. Both have serious limitations. Hosted models are vulnerable to a number of model inversion or inference attacks (*e.g.* [9,32,36]), while model licensing requires a robust and persistent proof of model ownership.

DNN watermarks [5,33,41] are designed to address the need for proof of model ownership. A robust watermark should provide a persistent and unforgeable link between the model and its owner or trainer. Such a watermark would require three properties. *First*, it needs to provide a strongly verifiable link between an owner and the watermark (*authentication*). *Second*, a watermark needs to be persistent, so that it cannot be corrupted, removed or manipulated by an attacker (*persistence*). *Finally*, it should be unforgeable, such that an attacker cannot add additional watermarks of their own to a model in order to dispute ownership (*piracy-resistance*).

Despite a variety of approaches, current proposals have failed to achieve the critical property of piracy resistance. Without it, a user of the model can train their own “valid” watermark into an already watermarked model, effectively claiming ownership while preserving the model’s classification accuracy. Specifically, recent work [37] showed that regularizer-based watermarking methods [5,6,33] were all vulnerable to piracy attacks. More recent watermark designs rely on embedding classification artifacts into models [1,41]. Unfortunately, our own experiments show that both techniques can be overcome by successfully embedding pirate watermarks with moderate training.

But what makes piracy resistance so difficult to achieve? The answer is that neural networks are designed to accept incremental training and fine-tuning. DNNs can be fine-tuned with existing training data, trained to learn or unlearn specific classification patterns, or “retargeted” to classify input to new labels via transfer learning. In fact, existing designs of DNN watermarks rely on this incremental training property to embed themselves into models. Thus, it is unsurprising that with additional effort, an attacker can use the same mechanism to embed more watermarks into an already watermarked model.

In this work, we propose *null embedding*, a new approach for embedding piracy-resistant watermarks into deep neural networks. Null embedding does not rely on incremental training. Instead, it can only be trained into a model at time of initial model training. Formally speaking, a null embedding (parameterized by a bit string) imposes an additional constraint on the optimization process used to train a model’s normal

classification behavior, *i.e.* the classification rules used to classify normal input. As this constraint is imposed at time of initial model training, it builds strong dependencies between normal classification accuracy and the given null embedding parameter. After a model is trained with a given null embedding, further (incremental) training to add a new null embedding fails, because it generates conflicts with the existing null embedding and destroys the model’s normal classification accuracy.

Based on the new null-embedding technique, we propose a strong watermark system that integrates public key cryptography and verifiable signatures into a bit-string embedded as a watermark in a DNN model. The embedded bit string inside a watermarked model is easily identified and securely associated with the model owner. The presence of the watermark does not affect the model’s normal classification accuracy. More importantly, attempts to train a different, pirate watermark into a watermarked model would destroy the model’s value, *i.e.* its ability to classify normal inputs. This deters any piracy attacks against watermarked models.

Our exploration of the null-embedding watermark produces several key findings, which we summarize below:

- We define the property of piracy resistance for DNN watermarks, and empirically confirm that existing approaches are vulnerable to piracy attacks.
- We validate the null-embedding technique and associated watermark on six classification tasks and different model architectures, extending beyond image classification to speech and human activity recognition. We show that piracy attacks against our watermarked models actually destroy model classification properties, and are no better than training the model from scratch, regardless of computation effort (§5.1, §7.3). We also confirm that our watermarks achieve all basic watermark properties (§7.4).
- We show that watermarked models are amenable to transfer learning systems: models can learn classification of new labels without losing their watermark properties (§8).
- With respect to countermeasures, we show our watermarks cannot be removed by modifications such as model fine-tuning, neuron pruning, model compression, or backdoor detection methods (§9.1, §9.2). They disrupt the model’s normal classification before they begin to have any impact on the watermark. We discuss model extraction attacks, and explore their limited benefits and practical costs using empirical results (§9.3).

Overall, our empirical results show that null-embedding shows promise as a way to embed watermarks that resist piracy attacks. We discuss limitations and future work in §10.

2 Related Work

The goal of watermarking is to add an unobtrusive and tamper-resistant signal to the host data, such that it can be reliably recovered from the host data using a recovery key.

As background, we now summarize existing works on digital watermarks, which have been well studied for multimedia data and recently explored for deep neural networks.

2.1 Digital Watermarks for Multimedia Data

Watermarking multimedia data has been widely studied in the literature (*e.g.* a survey [12]). A watermark can be added to *images* by embedding a low-amplitude, pseudorandom signal on top of the host image. To minimize the impact on the host, one can add it to the least significant bits of grayscale images [34], or leverage various types of statistical distributions and transformations of the image (*e.g.* [3, 15, 30]). For video, a watermark can take the form of imperceptible perturbations of wavelet coefficients for each video frame [27] or employ other perception measures to make it invisible to humans [38]. Finally, watermarks can be injected into audio by modifying its Fourier coefficients [3, 28, 31].

2.2 Digital Watermarks for DNNs

Recent works have examined the feasibility of injecting watermarks into DNN models. They can be divided into two groups based on the embedding methodology.

Weights-based Watermarks. The first group [5, 6, 33] embeds watermarks directly onto model weights, by adding a regularizer containing a statistical bias during training. But anyone knowing the methodology can extract and remove the injected watermark without knowing the secret used to inject it. For example, a recent attack shows that these watermarks can be detected and removed by overwriting the statistical bias [37]. Another design [8] enables “ownership verification” by adding special “passport” layers into the model, such that the model performs poorly when passport layer weights are not present. This design relies on the secrecy of passport layer weights to prove model ownership. Yet the paper’s own results show attackers can reverse engineer a set of effective passport layer weights. Since there is no secure link between these weights and the owner, attackers can reverse engineer a set of valid weights and claim ownership.

Query-based Watermarks. DAWN [29] proposes to protect an online, proprietary model by selectively mislabeling query responses. If an attacker attempts a model extraction attack against the hosted model, these modified responses leave a detectable “mark” inside the new model. This is used as a “watermark” to prove that the model was stolen.

Classification-based Watermarks. The second approach embeds watermarks in model classification results. Recent work [41] injects watermarks using the backdoor attack method, where applying a specific “trigger” pattern (defined by the watermark) to any input will produce a model misclassification to a specific target label. However, backdoor-based watermarks can be removed using existing backdoor defenses (*e.g.* [35]), even without knowing the trigger. Furthermore, this proposal provides no verifiable link between

the trigger and the identity of the model owner. Any party who discovers the backdoor trigger in the model can claim they inserted it, resulting in a dispute of ownership.

Another work [1] uses a slightly different approach. It trains watermarks as a set of classification rules associated with a set of self-engineered, abstract images only known to the model owner. Before embedding this (secret) set of images/labels into the model, the owner creates a set of commitments over the image/label pairs. By selectively revealing these commitments and showing that they are present in the model, the owner proves their ownership.

3 Problem Context and Threat Model

To provide context for our later discussion, we now describe the problem setting and our threat model.

Ownership Watermark. Our goal is to design a robust *ownership watermark*, which proves with high probability that a specific watermarked DNN model was created by a particular owner O . Consider the following scenario. O plans to train a DNN model F_θ for a specific task, leveraging significant resources to do so (e.g. training data and computational hardware). O wishes to license or otherwise share this valuable model with others, either directly or through transfer learning, while maintaining ownership over the intellectual property that is the model. If ownership of the model ever comes into question, O must prove that they and only they could have created F_θ . To prove their ownership of F_θ on demand, O embeds watermark \mathbb{W} into the model simultaneously when training the model. This watermark needs to be robust against attacks by a malicious adversary Adv .

Threat Model. At a high level, the adversary Adv wants to stake its own ownership claims on F_θ or at least destroy O 's claims. We summarize possible adversary goals as follows:

- **Corruption:** Adv corrupts or removes the watermark \mathbb{W} , making it unrecognizable and removing O 's ownership claim.
- **Piracy:** Adv adds its own watermark \mathbb{W}_A so it can assert its ownership claim alongside O 's.
- **Takeover:** A stronger version of piracy is that Adv replaces \mathbb{W} with its own watermark \mathbb{W}_A , in order to completely take over ownership claims of the model.

We make three assumptions about the adversary. *First*, we assume the owner makes the watermark procedure public and known to all, and Adv will follow the same procedure in trying to claim ownership of the model. *Second*, Adv is not willing to sacrifice model functionality, *i.e.* the attack fails if it dramatically lowers the model's normal classification accuracy. *Third*, Adv has limited training data and finite computational resources. If Adv has as much or even more training data as O , then it would be easier to train its own model from scratch, making ownership questions over F_θ irrelevant. We assume finite resources, because at some point, trying to compromise the watermark will be more costly in terms of

computational resources and time than training a model from scratch. Our goal is to make compromising a watermark sufficiently difficult, such that it is more cost-efficient for an adversary to pay reasonable licensing costs instead.

4 Understanding Piracy Resistance

While *piracy resistance* is a critical requirement for DNN watermarks, it is not addressed in prior work. To the best of our knowledge, all existing works are vulnerable to piracy attacks. In this section, we empirically validate this vulnerability, discuss why existing designs fail to achieve piracy resistance, and propose an alternative design.

4.1 The Need for Piracy Resistance

In an *ownership piracy* attack, an attacker attempts to embed their watermark into a model that is already watermarked. If the attacker can successfully embed their watermark into the watermarked model, the owner's watermark can no longer prove their (unique) ownership. That is, the ambiguity introduced by the presence of multiple watermarks invalidates the true owner's claim of ownership. To be effective, a DNN watermark *must* resist ownership piracy attacks.

4.2 Existing Works are Not Piracy Resistant

We show that, unfortunately, all existing DNN watermarking schemes are vulnerable to ownership piracy attacks.

Piracy Resistance of Weights-based Watermarks. Recent work [37] already proves that regularizer-based watermarking methods [5,6,33] are vulnerable to ownership piracy attacks, *i.e.* an attacker can inject new watermarks into a watermarked model without compromising the model's normal classification performance. Furthermore, the injection of a new watermark will largely degrade or even remove the original watermark. Another watermark design in this category [8] also fails to achieve piracy resistance because it cannot securely link an embedded watermark to the model owner. An attacker can demonstrate the existence of a pirate watermark without embedding it into the model.

Piracy Resistance of Query-based Watermarks. While DAWN [29] could "mark" models (re)created using a model extraction attack, it cannot prevent adversaries from inserting an *additional* mark to dispute model ownership. DAWN states that if more than one marks are found in a model, ownership will default to the mark that was registered first. However, if the attacker registers their mark before the true owner registers theirs, the attacker succeeds in pirating the model.

Piracy Resistance of Classification-based Watermarks. In the following section, we show empirically that existing works [1, 41] are vulnerable to piracy attacks. We follow the original papers [1, 41] to re-implement the proposed watermarking schemes on four classification tasks (MNIST,

Task	Watermark Design [1]			Watermark Design [41]		
	Normal Classification	Original Watermark (%)	Pirate Watermark (%)	Normal Classification (%)	Original Watermark (%)	Pirate Watermark (%)
MNIST	98.5 ± 0.0 / 97.4 ± 0.0	100.0 ± 0.0 / 48.8 ± 0.4	93.0 ± 0.0	98.6 ± 0.1 / 98.5 ± 0.1	100.0 ± 0.0 / 100.0 ± 0.0	100.0 ± 0.0
YTFaces	98.4 ± 0.5 / 95.4 ± 0.8	99.8 ± 0.7 / 53.3 ± 6.1	98.0 ± 0.0	98.4 ± 0.2 / 98.1 ± 0.2	100.0 ± 0.0 / 83.2 ± 34.4	100.0 ± 0.0
GTSRB	96.0 ± 0.1 / 95.7 ± 0.1	100.0 ± 0.0 / 98.0 ± 0.0	98.0 ± 0.0	96.1 ± 0.1 / 96.0 ± 0.2	100.0 ± 0.0 / 100.0 ± 0.0	100.0 ± 0.0
CIFAR-10	84.7 ± 0.2 / 84.0 ± 0.2	100.0 ± 0.00 / 98.2 ± 1.47	98.0 ± 0.0	86.0 ± 0.4 / 85.6 ± 0.3	100.0 ± 0.0 / 100.0 ± 0.0	100.0 ± 0.0

Table 1: Performance of watermarked models for four classification tasks. We show the before / after a piracy attack results in the table. The metrics are model classification accuracy on normal inputs, classification accuracy of the original (or owner) watermark, and classification accuracy of the pirate watermark. These results show that, for both watermark designs, an attacker can successfully insert a new, verifiable pirate watermark on a watermarked model.

YTFaces, GTSRB, and CIFAR-10)¹. Details of these tasks are listed in §7.1. Additional details concerning the DNN model architectures, training parameters, and watermark triggers used in our experiments can be found in the Appendix A.

To implement piracy attacks, we assume a strong attacker who has access to 5,000 original training images and the watermarked model. The goal of the attacker is to inject a new, verifiable pirate watermark into the model. This is achieved by the attacker updating the model using training data related to the pirate watermark. We found that for all four DNN models, a small number of training epochs is sufficient to successfully embed the pirate watermark. For both [41] and [1], MNIST, GTSRB, and CIFAR-10 only need 10 epochs while YTFaces only needs 1 epoch.

To evaluate each method’s piracy resistance, we use three metrics: (1) the model’s normal classification accuracy, (2) its classification accuracy on the original (owner) watermark, and (3) its classification accuracy on the pirate watermark. We record these before and after the piracy attack to measure the impact of the attack. In an ideal watermark design, no piracy attack should be able to successfully embed a pirate watermark into a model while maintaining its classification accuracy for normal inputs.

We list the results in Table 1. For both watermark designs, piracy attacks succeed (are recognized consistently) across all four classification tasks, and introduce minimal changes to the normal classification accuracy. For some models, the piracy attack also heavily degrades the original watermark. These results show that existing watermark designs are vulnerable to piracy attacks.

Note on the Piracy Claim in [1]. [1] assumes that the adversary uses the same number of watermark training epochs as the model owner, and applies an *additional verification step* via fine tuning, and claims the original watermark is more robust against fine-tuning than the pirate watermark. For completeness, we perform additional tests that reproduce the exact experimental configuration (same number of original/pirate watermark training epochs, followed by 10 epochs of fine-tuning) as [1]. Contrary to [1], our results show that across all four tasks, the pirate watermark is *more* robust to fine-tuning than the original watermark. For MNIST, CIFAR-10, and GTSRB, the pirate watermark’s classification

accuracy remains on average $82\% \pm 3\%$ after fine-tuning, while the accuracy of the original watermark drops to $57\% \pm 2\%$.

4.3 Rethinking Piracy Resistance

The key obstacle to piracy resistance is the *incremental trainability* property inherent to DNN models. A pretrained model’s parameters can be further tweaked by fine-tuning the model with more training data. Such fine-tuning can be designed to not disturb the foundational classification rules used to accurately classify normal inputs, but change fine-grained model behaviors beyond normal classification, *e.g.* adding new classification rules related to a backdoor trigger.

Existing Watermark Methodology: Separating Watermark from Normal Classification. Existing watermark designs, particularly classification-based watermarks, leverage the *incremental trainability* property to inject watermarks. In these designs, the model’s normal classification behaviors are made *independent* of the watermark-specific behaviors. Thus, the foundational classification rules learned by the model to classify normal inputs will not be affected by the embedded watermark. Such independence or isolation allows an adversary to successfully embed new (pirate) watermarks into the model without affecting normal classification.

Our New Methodology: Using Watermark to Control Normal Classification. Instead of separating watermark from normal classification, we propose to use the ownership watermark to constrain (or regulate) the generation/optimization of normal classification rules. Furthermore, this constraint is imposed at time of initial model training, creating strong dependencies between normal classification accuracy and the specific bit string in the given watermark. Once a model is trained / watermarked, further (incremental) training to add a new (pirate) watermark will break the model’s normal classification rules. Now the updated model is no longer useful, making the piracy attack irrelevant.

A stubborn adversary can continue to apply more training to “relearn” normal classification rules under the new constraint imposed by the pirate watermark. Yet the corresponding training cost is significantly higher (*e.g.* by a factor of 10 in our experiments) than training the model (and adding the pirate watermark) from scratch. Such significant (and unnecessary) cost leaves no incentive for piracy attacks in practice.

¹Both [1,41] design and evaluate watermarks for image-based classification tasks including CIFAR-10 and MNIST.

5 Piracy Resistance via Null Embedding

Following our new methodology, we now describe “null embedding”, an effective method to implement watermark-based control on the generation of normal classification rules. In a nutshell, null embedding adds a global, watermark-specific optimization constraint on the search for normal classification rules. This effectively projects the optimization space for normal classification to a watermark-specific area. Since different watermarks create different constraints and thus projections of optimization space, embedding a pirate watermark to a watermarked model will create conflicts and break the model’s normal classification.

In this section, we describe the operation of null embedding and its key properties that allow our watermark to achieve piracy resistance. Then, we show that a practical DNN watermark needs to be “dual embedded” (via both true and null embedding) into the model to achieve piracy resistance and be effectively verified and linked to the owner.

Without loss of generality, we describe both null embedding and our watermark design for CNN-based image classification tasks. Here the input to the model is an image. Our design can potentially be generalized to other classification tasks where the input to the classification model is a matrix. Later in §7 we implement and evaluate six classification tasks including image classification, speech recognition, and human activity recognition via accelerometer data, showing that our proposed watermark design can be successfully applied to all of them.

5.1 Null Embedding

Given a watermark sequence (e.g. a 0/1 bit string), the process of null embedding uses this sequence to modify the effective optimization space used to train the model’s normal classification rules. This is achieved by imposing a constraint during training, preventing a specific configuration on model inputs from affecting the normal classification outcome. To do so, null embedding must take place at the time of original model training. The model owner will start with an untrained model, generate extra training data related to null embedding, and train the model using the original and extra training data.

We formally define the process as follows. Let $\mathbf{F}_\theta : \mathbb{R}^N \rightarrow \mathbb{R}^M$ be a DNN model that maps an input $x \in \mathbb{R}^N$ to an output $y \in \mathbb{R}^M$. Let a watermark pattern p be a filter pattern applied to an image. Two samples are shown in Figure 1. Each filter pattern is defined by the placements of the black (0) and white (1) pixels on top of the gray background pixels (-1).

Definition 1 (Null Embedding) Let λ be a very large positive value ($\lambda \rightarrow \infty$). A filter pattern p is successfully null-embedded into a DNN model \mathbf{F}_θ iff

$$\mathbf{F}_\theta(x \oplus [p, \lambda]) = \mathbf{F}_\theta(x) = y, \quad \forall x \in \mathbb{R}^N, \quad (1)$$

where y is the true label of x . Here $x \oplus [p, \lambda]$ is an input filter operation. For each white (1) pixel of p , it replaces the pixel

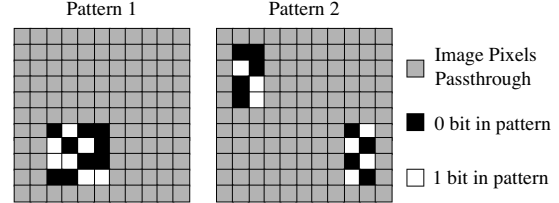


Figure 1: Two examples of a null embedding pattern. For each filter pattern, the color of a pixel represents the value of that pixel in the filter: gray means no change (value -1), black means 0 and white means 1. Each filter pattern is defined by the spatial distribution of the black/white pixel areas and the bit pattern in each black/white area.

of x at the same position with λ ; for each black (0) pixel of p , it replaces the corresponding pixel of x with $-\lambda$; the rest of x ’s pixels remain unchanged.

This shows that when p is successfully null embedded into the model, changing a set of p -defined pixels on any input x to hold extreme values λ and $-\lambda$ would not change the classification outcome. This condition (and the use of extreme values) set a strong and deterministic constraint on the optimization process used to learn the normal classification rules. And by enforcing the constraint defined by (1), null embedding of a pattern p will project the model’s effective input-vs-loss space (i.e. the optimization landscape) into a sub-area defined by p .

Properties of Null Embedding. We show that null embedding displays two properties that help us design pirate resistant watermarks. We also verify these properties empirically.

Observation 1: When N_p , the number of white/black pixels in p , is reasonably small, null embedding p into a model does not affect the model’s normal classification accuracy.

Null embedding of p confines the model’s optimization landscape into a sub-area. As long as this sub-area is sufficiently large and diverse, one can train the model to reach the desired normal classification accuracy. Our hypothesis is that when N_p is reasonably small compared to the size of the input image, the sub-area defined by p would be sufficiently large and diverse to learn accurate normal classification.

We test this hypothesis on the same four image classification tasks used in §4 (MNIST, YTFaces, GTSRB, and CIFAR-10) and two non-image classification tasks (SSCD and WISDM). We find that for all of them, N_p can be as large as 10% of the total input size without causing noticeable impact on normal classification accuracy. For example, $N_p = 6 \times 6$ on 28×28 images results in only 0.1%-1.5% accuracy loss. One can potentially reduce this loss by optimizing the design of filter pattern, e.g. configuring white/black pixel area as irregular shapes, which we leave to future work.

Observation 2: Once a model is trained and null embedded with p , an adversary cannot null embed a pirate p'

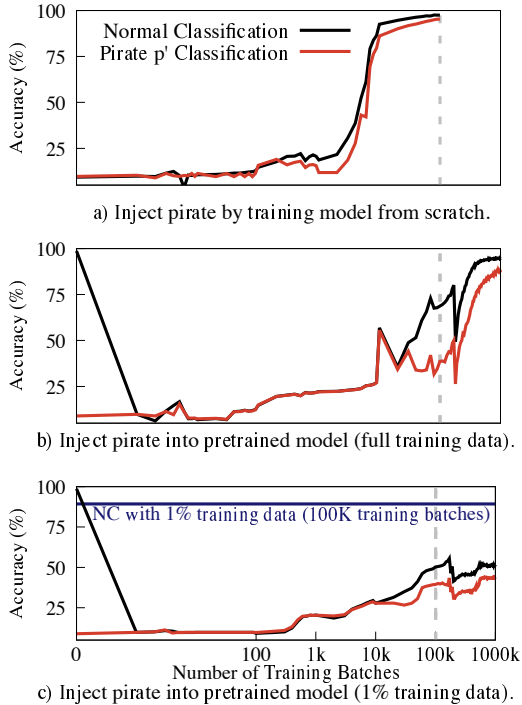


Figure 2: An instance of MNIST demonstrating the significant cost of piracy attack on null embedding. We plot the normal classification accuracy and pirate watermark p' 's classification accuracy under three scenarios: (a) injecting p' by training the model from scratch; (b) injecting p' into an watermarked-model using fine-tuning and full training data; and (c) same as (b) but using 1% of training data.

($p' \neq p$) without largely degrading the model's normal classification accuracy.

Our hypothesis is that null embedding of different patterns will create different projections of the optimization space. Once a model is successfully trained on p -based optimization space, any attempt to move it to a different optimization space (defined by p') will immediately break the model.

We verify this hypothesis by studying a watermarked model's normal classification accuracy and pirate p' classification accuracy as the adversary fine-tunes the model to embed p' . Our key finding is that embedding p' to a watermarked-model requires significantly more computation than training a model from scratch to embed p' .

An example trace on MNIST is shown in Figure 2, where we compare three scenarios to add a watermark p' to a model. These are: (a) the adversary trains the model *from scratch* and injects p' , (b) the adversary finds a watermarked model, fine-tunes the model to inject p' , using all the training data, and (c) which is the same as (b) except it uses 1% of the training data. Here we plot the training cost as the number of training batches (rather than epochs) to illustrate a fine-trained model behavior. Under scenario (a), the training takes 100k batches

to reach the proper accuracy levels. Under scenarios (b) and (c), the first few batches of fine-tuning immediately drop the normal classification accuracy to 10% (random guess). Even after 2k batches of fine-tuning, both normal and p' 's classification accuracies are still low. To reach the same accuracy as (a), the adversary will need 10x more training cost even when having the full training data (see Figure 2 (b)). When having 1% of training data (Figure 2 (c)), the training cost is likely exponentially more, as 1000k batches can only reach half of the classification accuracy. For fairness, we also plot the normal classification accuracy for scenario (a) but trained using 1% of training data after 100K training batches.

The significant cost of piracy attack is due to the *unlearning-then-relearning* effect. The adversary must first train the model to *unlearn* existing classification rules trained on p , then *relearn* new normal classification rules trained on p' . This overhead makes piracy attacks impractical.

Generating Distinct Watermark Patterns. Our design achieves piracy resistance by assuming that different watermark patterns project the optimization space differently. In our design, we create distinct watermark patterns by varying the spatial distribution of the white/black pixel areas and the (0/1) bit pattern within these areas (e.g. the two samples patterns in Figure 1). We also choose N_p to be a moderate value to reduce the collision probability across watermark patterns. Finally, we couple the watermark generation with strong cryptographic tools (i.e. public-key signatures in §6.1), preventing any adversary from forging the model owner's watermark.

5.2 Integrating Null and True Embeddings

While enabling piracy resistance, a null embedding alone is insufficient to build effective DNN watermarks. In particular, we found that the verification of solely null embedding-based watermarks could produce some small false positives. One potential cause is that some input regions could naturally have little impact on classification outcome, leading to false detection of watermarks not present in the model.

Thus, we propose combining the null embedding with a *true embedding* (similar to the backdoor based embedding used by existing watermark designs). In this design, true embedding links the watermark pattern with a deterministic (thus verifiable) classification output independent of the input (i.e. the watermark is a trigger in a backdoor). Combined with null embedding, they effectively minimize false positives in watermark verification.

Dual Embedding. We integrate the two embeddings by assigning them complementary patterns. This ties the embeddings to the same watermark without producing any conflicts. Given a watermark pattern p , the null embedding uses p , while the true embedding uses $inv(p)$. Here $inv(p)$ does not change any gray pixels (-1) in p but switches each white pixel to a black pixel and vice versa. We refer to this combina-

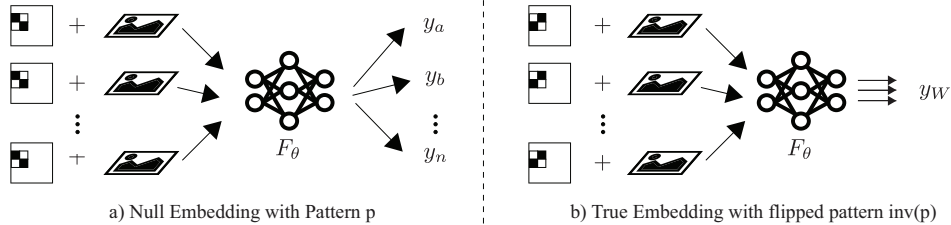


Figure 3: Our proposed dual embedding of a pattern p . (a) null embedding operates on the original pattern p , creating an input dependent classification output, forcing the model to train normal classification rules on the projected optimization space. (b) true embedding operates on the flipped pattern $\text{inv}(p)$, creating a deterministic classification output independent of the input. The dual embedding is integrated with the model training to simultaneously train and watermark the DNN model.

tion as *dual embedding* and formally define it below. Figure 3 illustrates dual embedding by its two components.

Definition 2 (Dual Embedding) Let λ be a very large positive value ($\lambda \rightarrow \infty$). A watermark pattern p is successfully dual embedded into a DNN model \mathbf{F}_θ iff $\forall x \in \mathbb{R}^N$,

$$\mathbf{F}_\theta(x \oplus [p, \lambda]) = \mathbf{F}_\theta(x) = y, \quad (2)$$

$$\mathbf{F}_\theta(x \oplus [\text{inv}(p), \lambda]) = y_w \neq y. \quad (3)$$

where y is the true label of x , and y_w is the watermark-defined label used by true embedding.

Our proposed true embedding teaches the model that the presence of a $[\text{inv}(p), \lambda]$ trigger pattern on any normal input x should result in the classification to the label y_w . Our design differs from existing work [41] in that it uses extreme values λ and $-\lambda$ to form the trigger. As such, our true embedding does not create anomalous (thus detectable) behaviors like traditional backdoors. As we will show in §9, the use of extreme values in our dual embedding makes our proposed watermark robust against model modifications, including existing backdoor defenses that attempt to detect and remove the watermark.

Simultaneous Dual Embedding and Model Training. A dual embedding must be fully integrated with the original model training process. The model owner, starting with an untrained model, generates extra training data related to both true and null embeddings, and trains the model using the original and extra training data. In this way, the model owner simultaneously trains and watermarks the target DNN model.

6 Detailed Watermark Design

To build a complete watermarking system, we apply digital signatures, cryptographic hashing, and existing neural network training techniques to generate and inject watermark patterns via dual embedding. Our design consists of the following three components:

The model owner generates the ownership watermark using her private key (§6.1). The model owner O uses its private key to sign some known verifier string v and generate

a signature (sig). Using sig , O applies deterministic hashing functions to produce her ownership watermark \mathbb{W} , defined by the filter pattern p , λ , and the true embedding label y_w .

The owner trains the model while injecting watermark (§6.2). O generates the corresponding training data for the dual embedding of \mathbb{W} . O combines these new training data with its original training data to train the model from scratch while embedding the watermark.

The authority verifying whether the ownership watermark \mathbb{W} is embedded in the model (§6.3). To prove its ownership, O provides its sig to a verification authority A . The verification takes two steps. A first verifies that sig is O 's signature using O 's public key and verifier string v . After verifying sig , A generates the watermark $\mathbb{W} = (p, y_w, \lambda)$ from sig , and verifies that \mathbb{W} exists in the model.

Next, we present detailed descriptions of each component.

6.1 Generating Ownership Watermark

The model owner O runs Algorithm 1 to generate its ownership watermark $\mathbb{W} = (p, y_w, \lambda)$.

Algorithm 1 Generating Ownership Watermark

- 1: $\text{sig} = \text{Sign}(O_{pri}, v)$
 - 2: $(p, y_w, \lambda) = \text{Transform}(\text{sig})$
-

First, O applies the $\text{Sign}(\cdot)$ function to produce a signature sig , taking the input of O 's private key O_{pri} and a verifier string v (a string concatenation of O 's unique identifier and a global timestamp). We implement $\text{Sign}(\cdot)$ using the common RSA public-key signature.

Next, O runs the $\text{Transform}(\cdot)$ function, a deterministic, global function for watermark generation with input sig (shown in Algorithm 2). Our implementation applies four hash functions h_1, h_2, h_3, h_4 to generate the specific pattern of the ownership watermark: the filter pattern p , the true embedding label y_w and the extreme value λ . The hash functions can be any secure hash function – we use SHA256. Here we assume p contains a single white/black pixel area of size $n \times n$. We represent p by the bit pattern $\text{bit}(p)$ in the white/black square, and the top-left pixel position of the

white/black square, $pos(p)$. This easily generalizes to cases where p contains multiple white/black areas.

Algorithm 2 $(p, y_W, \lambda) = \text{Transform}(sig)$

- 1: $H =$ height of input x
 - 2: $W =$ width of input x
 - 3: $Y =$ total number of model classes
 - 4: $y_W = h_1(sig) \bmod Y$
 - 5: $bit(p) = h_2(sig) \bmod 2^{n^2}$
 - 6: $pos(p) = [h_3(sig) \bmod (H - n), h_4(sig) \bmod (W - n)]$
 - 7: $\lambda = 2000$
-

Our watermark generation process can effectively prevent any adversary from forging the model owner’s watermark. To forge the owner’s watermark, the attacker must either forge the owner’s cryptographic signature or randomly produce a signature whose hash produces the correct characteristics, *i.e.* reverse a strong, one-way hash. Both are known to be computationally infeasible under reasonable resource assumptions.

6.2 Training Model & Injecting Watermark

Given $\mathbb{W} = (p, y_W, \lambda)$, O generates the watermark training data and labels corresponding to the dual embedding. O then combines the watermark training data with its original training data and uses loss-based optimization methods to train the model while injecting the watermark. In this case, the objective function for model training is defined as follows:

$$\underset{\theta}{\text{argmin}} \ell_{\mathbf{F}}(x, y) + \alpha \cdot \ell_{\mathbf{F}}(x \oplus [inv(p), \lambda], y_W) + \beta \cdot \ell_{\mathbf{F}}(x \oplus [p, \lambda], y)$$

where y is the true label for input x , $\ell_{\mathbf{F}}(\cdot)$ is the loss function for measuring the classification error (*e.g.* cross entropy), and α and β are the injection rates for true and null embedding.

6.3 Verifying Watermark

We start by describing the process of *private verification* where the third party verifier is a trusted authority, who keeps the verification process completely private (no leakage of any information). We then extend our discussion to *public verification* by untrusted parties.

Private Verification via Trusted Authority. The “claimed” owner O submits its signature sig , public key O_{pub} , and verifier string v to a trusted authority. The authority runs Algorithm 3 to verify whether O does have its ownership watermark embedded in the target model \mathbf{F}_{θ} . Here we assume that the trusted authority has access to the $\text{Transform}(\cdot)$ function (Algorithm 2) and will not leak the signature sig and the corresponding ownership watermark pattern.

The verification process includes two steps. *First*, the authority verifies that sig is a valid signature over v generated by the private key associated with O_{pub} (line 1 of Algorithm 3). This uniquely links sig to O . *Second*, the authority checks whether a watermark defined by sig is injected into the model

Algorithm 3 Private Verification of Ownership Watermark

- 1: **if** not $\text{Verify}(O_{pub}, sig, v)$ **then**
 - 2: Verification fails.
 - 3: **else**
 - 4: $(p, y_W, \lambda) = \text{Transform}(sig)$
 - 5: $\Phi_{null} = Pr(\mathbf{F}_{\theta}(x \oplus [p, \lambda]) = \mathbf{F}_{\theta}(x) = y)$
 - 6: $\Phi_{true} = Pr(\mathbf{F}_{\theta}(x \oplus [inv(p), \lambda]) = y_W)$
 - 7: **if** $\min(\Phi_{true}, \Phi_{null}) > T_{watermark}$ **then**
 - 8: Verification passes.
 - 9: **else**
 - 10: Verification fails.
 - 11: **end if**
 - 12: **end if**
-

\mathbf{F}_{θ} . To do so, it first runs $\text{Transform}(sig)$ to generate the ownership watermark (p, y_W, λ) (line 4 of Algorithm 3). The authority forms a test input set, and computes the classification accuracy of the null embedding (line 5 of Algorithm 3) and true embedding (line 6 of Algorithm 3). If both accuracies exceed the threshold $T_{watermark}$, the authority concludes that the owner’s watermark is present in the model. Ownership verification succeeds.

Public Verification. The above private verification assumes the authority can be trusted not share information about the watermark pattern. If the pattern is leaked to an adversary, the adversary can attempt to modify/corrupt the watermark by applying a small amount of training to change the classification outcome of dual embedding $(x \oplus [p, \lambda])$ and/or $x \oplus [inv(p), \lambda]$, so that $\min(\Phi_{true}, \Phi_{null})$ drops below $T_{watermark}$. The result is a new model where the ownership watermark is no longer verifiable. This is the *corruption* attack (not piracy attack) mentioned in §3.

This issue can be addressed by embedding multiple watermarks in the model while only submitting one watermark to the trusted authority. As a result, any hidden or “unannounced” watermark will not be leaked. Should a dispute arise, the owner can reveal one hidden watermark to prove ownership. We have experimentally verified that multiple, independently generated watermarks can be simultaneously added at initial training time into practical DNN models (listed in §7) without degrading model accuracy.

7 Experimental Evaluation

In this section, we use empirical experiments on six classification tasks to validate our proposed watermark design.

7.1 Experimental Setup

To cover a broad array of settings, we consider six classification tasks, from image recognition, speech recognition to human activity recognition. These tasks target disjoint subjects and employ different model architectures. In the following, we briefly describe each task, its dataset and classi-

Task	Dataset	# Classes	Training data size	Test data size	Input size	Model architecture
Digit Recognition (MNIST)	MNIST	10	60,000	10,000	(28, 28, 1)	2 Conv + 2 Dense
Face Recognition (YTFaces)	YouTube Faces	1,283	375,645	10,000	(55, 47, 3)	4 Conv + 1 Merge + 1 Dense
Traffic Sign Recognition (GTSRB)	GTSRB	43	39,209	12,630	(48, 48, 3)	6 Conv + 3 Dense
Object Recognition (CIFAR-10)	CIFAR-10	10	50,000	10,000	(32, 32, 3)	6 Conv + 3 Dense
Speech Recognition (SSCD)	SSCD - Digits	10	9,782	988	(129, 71, 1)	2 Conv + 2 Dense
Human Activity Recognition (WISDM)	WISDM	6	20,868	6,584	(80, 3)	4 Conv + 3 Dense

Table 2: Overview of classification tasks with their associated datasets and DNN models.

fication model (also summarized in Table 2). Further details on model structures (Tables 9-14) and training hyperparameters (Table 16) are listed in the Appendix.

- Digit Recognition (MNIST [17]) classifies images of handwritten digits to one of ten classes. Each image is normalized so the digit appears in the center. The classification model has two convolutional layers and two dense layers.
- Face Recognition (YTFaces [22, 24]) is to recognize the faces of 1,284 people. These faces are drawn from a large (3,425) set of YouTube videos. Each person in the target dataset has at least 100 labeled images. The corresponding facial recognition model is the DeepID model [26].
- Traffic Sign Recognition (GTSRB [25]) identifies 43 types of traffic signs based on the German Traffic Sign Benchmark (GTSRB) dataset. The classification model contains six convolutional layers and three dense layers.
- Object Recognition (CIFAR-10 [14]) identifies objects in images as one of ten object types. It uses the CIFAR-10 dataset with 60,000 color images in 10 classes (6,000 images per class). The classification model has six convolutional layers and three dense layers.
- Speech Recognition (SSCD [4]) classifies audio samples of ten digits 0 - 9. It uses the Synthetic Speech Command Dataset (SSCD), with 9,782 training audio samples and 988 test samples for the 10 classes. We pre-process each raw audio segment (.wav) into its spectrogram using the `scipy` Python library. The classification model has two convolutional layers and two dense layers.
- Human Activity Recognition (WISDM [16]) classifies accelerometer readings (time series of three-dimensional sensor data) into one of six human activities (Walking, Jogging, Stair Climbing, Sitting, Standing, and Lying Down). It uses the WISDM dataset with 20,868 training signals and 6,584 testing signals. The classification model has four convolutional layers and three dense layers.

For all tasks, we normalize the value of input to $[0, 1]$.

Watermark Configuration. We embed watermarks by setting the extreme value $\lambda = 2000$. For the first five tasks, a watermark pattern p is a 6×6 block in the input, representing the black/white area in Figure 1; for WISDM, we use a smaller 3×3 block since its input size is much smaller. In our experiments, we randomly vary the position and pattern of the black/white block to ensure that our results generalize. The watermark is added to a subset of training data during each training batch. The portion of the watermarked training data

defines the injection ratio. Table 16 lists the injection ratio for each task.

To verifying the presence of a watermark, we set $T_{watermark} = 80\%$, the threshold used by Algorithm 3. Here $T_{watermark}$ is set by first estimating the watermark classification accuracy using a validation set (from the training data), and choosing a value that is (slightly) lower than the observed accuracy.

Attacker Configuration. As described in the threat model (§3), we assume attackers only have a limited subset of the original training data (because otherwise attackers could easily train their own model and have no need to pirate the owner’s model). For our experiments, the attacker has 5,000 images for MNIST, YTFaces, GTSRB, CIFAR-10 (the same configuration used in our evaluation of existing works in §4), and 2,000 samples for SSCD and WISDM, since they have fewer data.

Evaluation Metrics. We consider two metrics: normal classification accuracy and watermark classification accuracy. We further break down watermark accuracy into its true and null embedding components.

- **Normal Classification Accuracy (NC):** The probability that the classification result of any normal input x equals its true label y , *i.e.* $\Pr(\mathbf{F}_\theta(x) = y)$.
- **Watermark Classification Accuracy (WM):** The minimum classification accuracy of the true and null embedding, $\phi = \min(\phi_{true}, \phi_{null})$, where

$$\phi_{null} = \Pr(\mathbf{F}_\theta(x \oplus [p, \lambda]) = \mathbf{F}_\theta(x) = y), \quad (4)$$

$$\phi_{true} = \Pr(\mathbf{F}_\theta(x \oplus [inv(p), \lambda]) = y_W). \quad (5)$$

Note that we will examine the classification accuracy of both the owner watermark and the pirate watermark when we examine our watermark’s piracy resistance.

7.2 Overview of Experiments

We perform experiments to verify whether our proposed watermark design achieves piracy resistance (§7.3) and the four basic watermark requirements (§7.4). We also report the computation overhead for embedding and verifying the watermark (§7.5). Later in §8 and §9, we study the impact of transfer learning on our watermark, as well as adaptive attacks including model fine-tuning and compression, intentional efforts to corrupt/remove the ownership watermark, and model extraction.

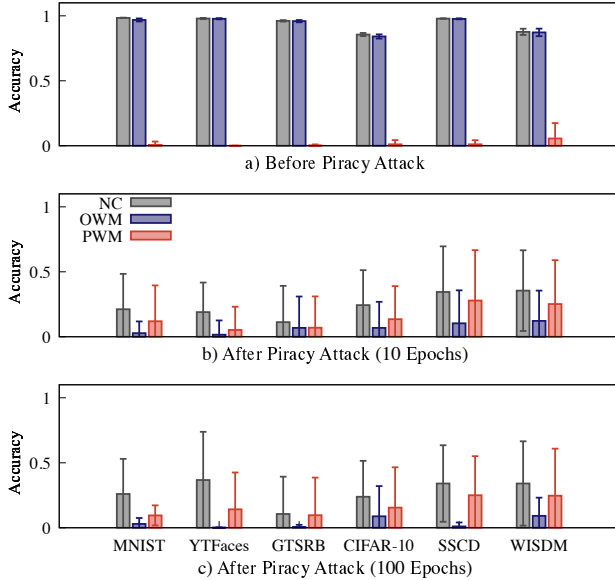


Figure 4: Analyzing piracy resistance: normal classification accuracy (NC), owner’s watermark accuracy (OWM) and pirate watermark accuracy (PWM) as an adversary attempts to embed a pirate watermark into a watermarked model. (a) before piracy attack; (b) after piracy attack using 10 training epochs (1 epoch for YTFaces); (c) after piracy attack using 100 training epochs.

7.3 Result: Piracy Resistance

We verify the piracy resistance of our watermark design by launching piracy attacks on watermarked models and studying its impact on the model. As discussed in §4, an adversary runs a piracy attack by fine-tuning a watermarked model to inject a new, pirate watermark. Here we assume that the owner’s watermark and the pirate watermark have the same black/white block size: *i.e.* $N_p = 3 \times 3$ for WISDM and $N_p = 6 \times 6$ for all other tasks.

We evaluate two scenarios:

- A direct comparison with existing watermark designs [1, 41], by evaluating our watermark design using the same² piracy attack configuration used in §4. Recall that our results in Table 1 in §4 show that existing designs fail to resist piracy attacks.
- An extended scenario where the adversary uses more training batches (*e.g.* 100 epochs rather than 10 epochs) to inject the pirate watermark.

Our Design vs. Existing Watermark Designs. Figure 4a and 4b plot the normal and watermark classification accuracies of a watermarked model (using our design), before and after the piracy attack, respectively. For each task, we create 10 owner-watermarked models (using randomly chosen owner watermark patterns), and test 50 randomly generated

²As stated in §4, we inject the pirate watermark using 1 training epoch for YTFaces and 10 training epochs for all other tasks, use the last learning rate from the original model training and the same configurations of the original model training listed in Table 16 (see Appendix)

pirate watermarks on each model. Consequently, for each task, we have 10 before-attack instances and 500 after-attack instances. We report the average and standard deviation. The presence of non-zero values for pirate watermark accuracy *before* the pirate attack comes from a model’s propensity to randomly guess the class for unknown inputs. These values approximate $1/N$, where N is the number of classes, and are far lower than the verification threshold $T_{watermark}$.

We observe a consistent pattern across all six tasks – after the piracy attack, both the normal classification accuracy and the owner watermark accuracy drop significantly from a high value (87%-99%) down to a low value (11%-36% for normal, 2%-12% for owner watermark). That is, as the piracy attack reduces the trace of the owner watermark (to inject the pirate watermark), it also destroys the model, making the model useless for the target classification task. This again demonstrates the strong tie between the owner watermark and the normal classification. Another observation is that even after 10 epochs of training (fine-tuning), the adversary still cannot embed the pirate watermark (the average classification accuracy of the pirate watermark is only 5%-28% and close to random guess). We also verified that using a smaller learning rate does *not* improve pirate watermark accuracy³. These results show that our proposed watermark design can resist piracy attacks that existing designs fail to resist.

Ineffectiveness of Adding More Training Batches. After the adversary spends 100 training epochs to inject the pirate watermark, Figure 4(c) plots the normal classification accuracy, and two watermarks’ classification accuracies. As expected, adding 10x more training batches improves the normal classification accuracy and the pirate watermark accuracy, but the amount of improvement is small in general and even invisible for some tasks. More importantly, even after spending 100 training epochs, both the normal classification accuracy and pirate watermark accuracy are still low. In this case, the classification model is broken and the pirate watermark fails the verification.

Summary. These results show that an adversary *cannot* inject its pirate watermark without breaking the model’s classification capability. As a piracy attack applies model fine-tuning to corrupt the owner’s watermark, it also renders the updated model useless by drastically degrading the normal classification accuracy. When a model no longer functions, the corresponding piracy attack becomes irrelevant.

7.4 Result: Basic Watermark Requirements

In addition to being piracy-resistant, our watermark design also fulfills the four basic requirements for watermarking:

³Tests on MNIST showed that using very small learning rates (10^{-5} , 10^{-6}) improves normal classification accuracy (to 91%-95%) but not pirate watermark accuracy (which remains around 13%-19%). Classification accuracy for the owner watermark stays at 85%-94%.

- 1) *functionality-preserving*, *i.e.* embedding a watermark does not degrade the model’s normal classification;
- 2) *effectiveness*, *i.e.* an embedded watermark can be consistently verified;
- 3) *non-trivial ownership*, *i.e.* the probability that a model exhibits behaviors of a non-embedded watermark is negligible;
- 4) *authentication*, *i.e.* there is a provable association between an owner and their watermark, so that an adversary cannot claim an embedded watermark as their own [33, 41];

We now describe our experiments verifying that our watermark design fulfills these requirements. Since we have shown that existing watermark designs [1, 41] are not piracy-resistant, we do not compare our work against them on these basic watermark requirements. Their failure to achieve the crucial property of piracy resistance makes their performance on other metrics irrelevant.

Functionality-preserving. In Table 3, we compare the normal classification (NC) accuracy of watermarked and watermark-free versions of the same model. Both versions are trained using the same configuration (Table 16 in Appendix), except (obviously) the watermark-free version is not trained on watermark-specific data. For each task, we train 10 watermark-free models and 10 watermarked models (each with a randomly generated watermark), and report the average performance with standard deviation. Across all six tasks, the presence of a watermark introduces minor impact on the normal classification accuracy ($-0.6\% \pm 1.5\%$).

Effectiveness. Using Algorithm 3, we verify that a watermark is present in a model by ensuring watermark classification accuracy is above the $T_{\text{watermark}} = 80\%$ threshold. We experiment with 10 random owner watermarks for each task and all can be reliably verified (as shown by the average watermark classification accuracy with standard deviation in Table 3). We also list the classification accuracy of the true and null watermark components. We see that true embedding has a higher classification accuracy since it produces a deterministic behavior independent of the input. Furthermore, by imposing constraints on normal classification rules (see eq. (1)), the null embedding’s accuracy depends heavily on that of normal classification. This explains why the null embed-

Task	Watermark-free Model	Watermarked Model			
	NC (%)	NC (%)	null (%)	true (%)	WM (%)
MNIST	98.7 ± 0.0	98.4 ± 0.2	96.8 ± 1.2	100.0 ± 0.0	96.8 ± 1.2
YTFaces	99.1 ± 0.1	97.8 ± 0.5	97.7 ± 0.5	100.0 ± 0.0	97.7 ± 0.5
GTSRB	96.4 ± 0.3	96.1 ± 0.5	95.9 ± 0.9	100.0 ± 0.0	95.9 ± 0.9
CIFAR-10	87.6 ± 0.2	85.6 ± 1.2	84.1 ± 1.6	100.0 ± 0.0	84.1 ± 1.6
SSCD	97.6 ± 0.2	97.9 ± 0.2	97.7 ± 0.4	100.0 ± 0.0	97.7 ± 0.4
WISDM	87.2 ± 1.4	87.7 ± 2.4	87.2 ± 2.9	100.0 ± 0.0	87.2 ± 2.9

Table 3: Analyzing basic watermark requirements: Normal classification (NC) and watermark classification accuracy (both true and null components) of watermark-free and watermarked models. We report the average results with standard deviation for 10 watermark-free models and 10 watermarked models.

Task	Using All Test Data		Using 1K Test Samples	
	Time (s)	WM (%)	Time (s)	WM (%)
MNIST	1.8 ± 0.2	96.6 ± 1.5	0.45 ± 0.1	97.3 ± 1.1
YTFaces	3.9 ± 0.4	97.7 ± 0.4	1.14 ± 0.1	97.4 ± 0.8
GTSRB	4.8 ± 0.3	95.9 ± 0.9	1.20 ± 0.2	96.3 ± 0.7
CIFAR-10	3.0 ± 0.2	84.1 ± 1.6	1.09 ± 0.2	84.6 ± 2.0
SSCD	0.6 ± 0.2	97.7 ± 0.4	-	-
WISDM	1.7 ± 0.2	87.2 ± 2.9	0.78 ± 0.1	86.7 ± 2.8

Table 4: Verification runtime and watermark classification accuracy with different number of samples used in verification. We report the average and standard deviation values across 10 watermarked models. Since SSCD has less than 1k test data, we omit its results of 1k samples.

ding’s accuracy is lower for CIFAR-10 and WISDM compared to the other four tasks.

Non-trivial ownership. We first empirically verify that a watermark-free model consistently fails the watermark verification test. For each task, we consider the above mentioned 10 watermark-free models. We then randomly generate 1000 different watermarks and run the watermark verification test to examine their presence on the model. For all six tasks, all verification tests fail, indicating a 0% false positive rate for watermark-free models, *i.e.*, our proposed watermark design achieves the non-trivial ownership property.

Authentication. Our watermark method satisfies the authentication requirement by design. To generate the ownership watermark in §6.1, we use a hash function that is both a strong one-way hash (*i.e.* difficult to reverse) and collision resistant (low probability of natural collisions). Compromising the watermark requires a third party to find a valid collision to the hash algorithm, and use that input to claim that they originated the watermark. Since our design uses a preimage-resistant hash (SHA256), such an attack is unrealistic.

7.5 Result: Overhead

We report the overhead of watermark injection and verification for our design in Figure 5 and Table 4, respectively.

Watermark Injection. Because an owner’s watermark is injected during model training, we evaluate the overhead of watermark injection by comparing the training time of watermarked models with their watermark-free counterparts. As before, we train 10 watermarked models and 10 watermark-free versions using the configurations in Table 16. For a fair comparison, we also compare the normal classification (NC) accuracy between the watermarked and watermark-free models, by varying the training time of the watermarked models.

Figure 5 plots the NC accuracy of a watermarked model normalized by its watermark-free version vs. the training time used for the watermarked model normalized by that of the watermark-free model. As is evident, watermarked models can achieve 95-100% of the watermark-free NC within 115% of the training time used by watermark-free models. This shows that our watermarking method introduces mini-

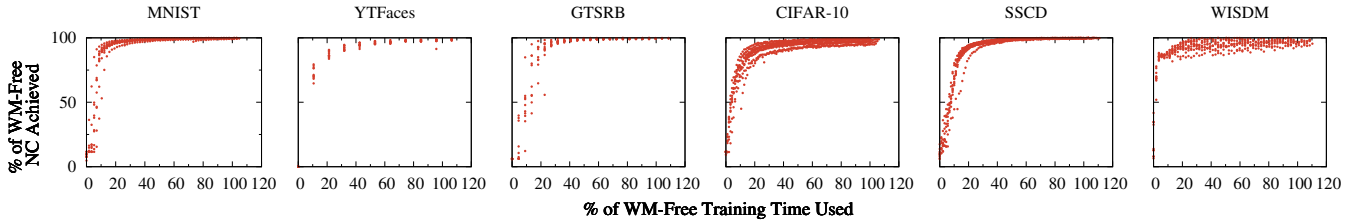


Figure 5: Analyzing watermark injection overhead: The % of WM-free model training time used for watermarked models to achieving certain % of WM-free NC achieved. The watermarked models can achieve over 95% of the average normal classification accuracy with in 115% of the average training time for WM-free models.

mal overhead into the model training process.

Watermark Verification. The verification process for our watermark method is fast ($< 5s$ for all models) if we use the entire test data (in Table 2) as the verification dataset, and can be further reduced to $\sim 1s$ if we use a subset of test data (1,000 samples). To demonstrate this, we show in Table 4 the verification runtime and the measured watermark accuracy for verification using the full test set and its 1K samples. We report the results as the average and standard deviation values over 10 different watermarked models. The verification process runs on one Intel(R) Core(TM) i9-7920X CPU @ 2.90GHz and one NVIDIA TITAN Xp.

8 Transfer Learning

Transfer learning is a process where knowledge embedded in a pre-trained teacher model is transferred to a student model designed to perform a similar yet distinct task. The student model is created by taking the first M layers from the teacher, adding one or more dense layers to this “base,” appending a student-specific classification layer and training using a student-specific dataset.

Next we show that transfer learning does not degrade our watermark. Specifically, we evaluate two watermark qualities related to transfer learning. First, a watermark (in the teacher model) should allow transfer learning, *i.e.* allow customization of student models with high accuracy. Second, a watermark should persist through the process, *i.e.* still be verified inside trained student models.

We implement a transfer learning scenario on a traffic sign recognition task. Our teacher task is German traffic sign recognition (GTSRB), and our student task is US traffic sign recognition. We use LISA [20] as our student dataset and follow prior work [7] in constructing the training dataset. We use two models trained on GTSRB as teacher models (a watermark-free model and a watermarked model). To create the student model, we copy all layers except last layer from the teacher model and add a final classification layer. We consider four different methods to train the student model: fine-tuning the added layers only, fine-tuning the last two dense layers, fine-tuning all dense layers and fine-tuning all layers. We train the student model for 200 epochs. More details of the training settings can be found in Appendix. For each set-

Fine Tuning Configuration	Watermark-free Model’s Student NC (%)	Watermarked Model’s Student NC (%)
Added Layers	79.1 ± 2.8	75.7 ± 1.4
Last Two Layers	86.1 ± 1.1	85.1 ± 1.7
All Dense Layers	90.9 ± 1.5	90.3 ± 1.0
All Layers	92.2 ± 0.4	93.4 ± 0.8

Table 5: Student model’s normal classification accuracy with watermark-free and watermarked models as teachers. We report the average results with standard deviation on 5 different models for each number.

Fine Tuning Configuration	Recovered NC (%)	null (%)	true (%)	WM (%)
Last Layer	95.8 ± 0.6	95.5 ± 1.2	100.0 ± 0.0	95.5 ± 1.2
Last Two Layers	96.0 ± 0.8	95.7 ± 1.2	100.0 ± 0.0	95.7 ± 1.2
All Dense Layers	95.8 ± 0.8	95.5 ± 1.3	100.0 ± 0.0	95.5 ± 1.3
All Layers	95.8 ± 0.5	92.9 ± 2.5	100.0 ± 0.0	92.9 ± 2.5

Table 6: The verification authority can reliably “recover” and verify the owner watermark from a student model trained on a watermarked teacher model, regardless of the fine-tuning method used by the transfer learning. Thus, despite the fact that transfer learning removes the watermark target label (y_w) from the student model, the teacher’s owner watermark is still embedded into the student model. We report the average results with standard deviation on 5 different models for each number.

ting, we repeat the experiments on 5 different watermarked models and report the mean with standard deviation.

Our watermark design allows transfer learning. Table 5 lists the normal classification accuracy of the student models trained from our two teacher models. We see that fine-tuning more layers during transfer increases student model’s normal classification accuracy. In fact, when all layers are fine-tuned, the watermarked student performs better than the one trained by a watermark-free model. Thus, our watermarked model can be used as a teacher model for transfer learning.

Our watermark persists through transfer learning. We now verify whether the original watermark in the teacher model can still be detected/verified in the student models. Here we consider the case where the target label y_w used by our watermark’s true embedding is removed by the transfer process. We show that while the absence of y_w in the student model “buries” the owner watermark inside the model, one can easily “recover” and then verify the owner watermark using a transparent process.

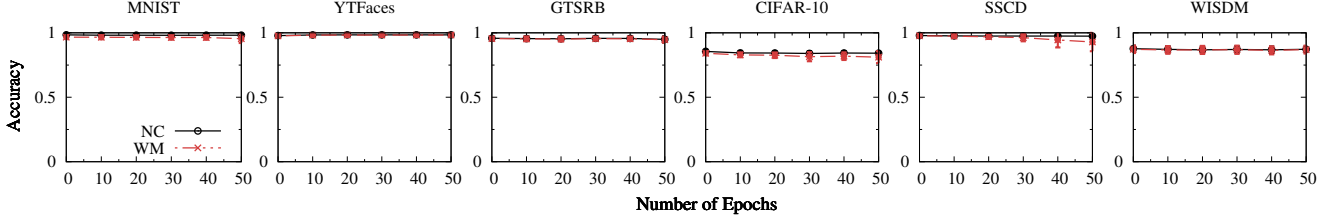


Figure 6: The model’s normal classification and watermark classification accuracy remain stable during model fine-tuning. NC and WM represent normal classification accuracy and watermark accuracy respectively. We report the average results with standard deviation of the performance over 10 different watermarked models for each task.

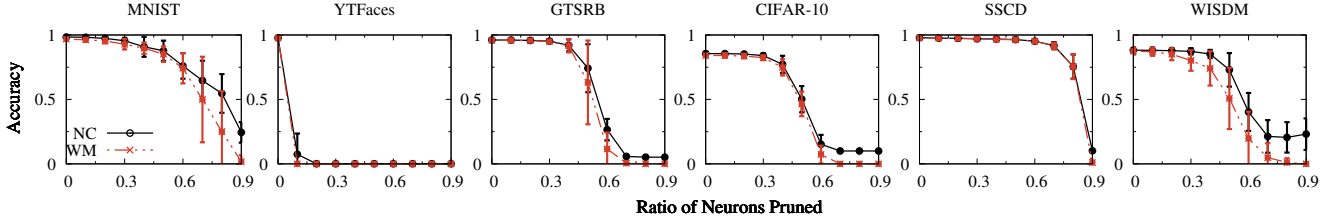


Figure 7: The impact of neuron pruning on the model’s normal classification (NC) and watermark classification accuracy (WM), as a function of the ascending pruning ratio. We report average results of the performance with standard deviation over 10 different watermarked models for each task.

Specifically, the verification authority first examines whether the student model contains y_W (defined by the owner watermark to be verified). If not, the authority first “recovers” the owner watermark from the student model. This is done by adding y_W to the student model and fine-tuning it for a few epochs using clean training data. Here the fine-tuning method is the same one used by the transfer learning⁴. The entire recovery process is transparent and can be audited by an honest third party.

We run the above verification process on the LISA student model generated from the watermarked teacher model. In this case, y_W (a German traffic sign) is not present in the student model. We replace the last layer of the student model with a randomly initialized layer whose dimensions match those of the teacher model’s final layer. This is our “recovered” teacher model. We fine tune the recovered model using the teacher’s training data for 3 epochs, and run the owner watermark verification on the model. Results in Table 6 shows that the owner watermark can be fully restored and reliably verified regardless of the transfer learning techniques used to train the student model. This confirms that our proposed watermark can persist through transfer learning.

9 Adaptive Attacks and Countermeasures

In this section, we evaluate our watermark’s robustness against three groups of adaptive attacks that an adversary can use to remove or corrupt an embedded watermark. These include (1) commonly used model modifications to improve accuracy and efficiency (§9.1), (2) known defenses to de-

tect/remove backdoors from the model (§9.2), and (3) model extraction attacks that create a watermark-free version of the model (§9.3).

9.1 Modifications for Accuracy and Efficiency

Model tuning techniques designed to improve accuracy or efficiency could impact embedded watermarks. We test the robustness of our watermarks against two types of modifications: (1) fine-tuning to improve accuracy; and (2) model compression via neuron pruning.

Fine-tuning for Accuracy. Fine-tuning is widely used to update model weights to improve normal classification accuracy. We test our watermark against fine-tuning, allowing weights in all model layers to be updated. We use the same parameters such as batch size, optimizer, and decay as the original model training, and the learning rate used during the original model training. Figure 6 plots normal classification and watermark classification accuracy (null, true) during fine-tuning. Even after 50 epochs of fine-tuning, the embedded watermark and the normal classification are not affected.

Neuron Pruning/Model Compression. Neuron pruning compresses a model by selectively removing neurons considered unnecessary for classification [10, 11]. An adversary can try to use neuron pruning to remove the watermark. We run the common neuron pruning technique (*ascending pruning*) [11], which first removes neurons with smaller absolute weights. Figure 7 shows the impact of pruning ratio on normal classification and watermark accuracy. Since the accuracy of null embedding is tied to normal classification accuracy, there is no reasonable level of pruning where normal classification is acceptable while the embedded watermark is disrupted. Our watermark design is robust against neuron pruning.

⁴One can determine the fine-tuning method used by the transfer learning by comparing the weights of student and teacher models and identifying the set of the layers modified by the transfer learning.

Task	Original Neural Cleanse		Customized Neural Cleanse	
	Original Model	Watermarked Model	Original Model	Watermarked Model
MNIST	1.8 ± 1.1	1.0 ± 0.3	2.0 ± 0.8	1.6 ± 0.5
YTFaces	2.0 ± 0.6	1.7 ± 0.3	2.1 ± 0.6	1.8 ± 0.4
GTSRB	2.1 ± 0.5	1.8 ± 0.3	1.9 ± 0.5	1.8 ± 0.4
CIFAR-10	1.3 ± 0.5	1.4 ± 0.6	1.5 ± 0.6	1.6 ± 0.6
SSCD	1.9 ± 0.9	1.8 ± 0.5	2.0 ± 0.6	1.8 ± 0.6
WISDM	0.9 ± 0.1	0.9 ± 0.1	0.9 ± 0.1	1.0 ± 0.1

Table 7: Anomaly index reported by Neural Cleanse when running on original (watermark-free) and watermarked models. Suggested threshold for detecting anomalies is 2 [35]. We report the average results with standard deviation for 10 watermarked models.

9.2 Backdoor Detection/Removal

The true embedding component of our watermark design is similar to a traditional neural network backdoor. Knowing this, an adversary may attempt to detect and remove it using existing backdoor defenses. We test this attack by applying the three most well-known methods for backdoor detection/removal: Neural Cleanse [35], ABS [19], and Fine-Pruning [18].

Neural Cleanse Neural Cleanse detects backdoors by searching for a small perturbation that causes all inputs to be classified to a specific label, and detecting it as an anomaly (e.g. whose anomaly index > 2). For reference, we also apply Neural Cleanse on the watermark-free version of our models.

Neural Cleanse is unable to detect any “backdoor” (aka watermark) on our watermarked models (see Table 7). Across all watermarked models, the anomaly index is lower than the threshold of 2, and often lower than that of the original (watermark-free) model. This is because Neural Cleanse (and followup work) assume that backdoors are *small* input perturbations that create large changes in the feature space. Since our true and null embeddings use extreme values $-\lambda$ and λ , they represent *large* perturbations in the input space (L2 distance) that do not register as anomalies.

To address this limitation, we develop an enhanced version (NeuralCleanse++) to handle extreme values. We enlarge the reverse engineer search space of Neural Cleanse from RGB space to $-\lambda$ and λ space, and rerun the above experiments. Table 7 shows the anomaly index of clean and watermark models under the customized Neural Cleanse. A small portion (6 out of 60) watermark models have anomaly index above 2, however, NeuralCleanse++ flagged more clean models (11 out of 60). We believe this is due to the existence of natural backdoors in a much larger search space, which lead to clean models to produce false positives. For watermarked models that show up as anomalies, the labels identified by NeuralCleanse++ as backdoor targets are incorrect. Thus NeuralCleanse++ is also ineffective at detecting and our watermark.

ABS. ABS [19] detects backdoors by iteratively stimulating internal model neurons and watching for abnormal model

Data	50k	100k
ImageNet	$92.8 \pm 2.1\%$	$94.0 \pm 1.3\%$
Youtube Faces	$73.2 \pm 6.9\%$	$78.7 \pm 7.1\%$
Random	$7.6 \pm 3.2\%$	$8.0 \pm 2.3\%$

Table 8: The normal classification accuracy of the substitute model built by the model extraction attack [21] using each of the three data sources. For each entry in the first row, we show # of (unlabeled) images used to train the substitute model. The target model’s normal classification accuracy is 96.1%. The size of original model training data is 39k.

output behaviors. If any neurons cause abnormal outputs, ABS reverse engineers backdoor triggers that optimally activate the neuron. We test ABS on 10 watermarked models and 10 watermark-free models for CIFAR-10⁵. ABS does not detect any of our watermarks in any models.

Fine-Pruning Fine-pruning [18] proposes to first prune the model with some neurons and then use data to fine-tune the pruned model for several epochs to remove backdoors. We implement fine-pruning on our watermarked models for all tasks. We prune 10%, 30%, 50% and 70% of the neurons in the last convolutional layer of the model as suggested by [18] and fine-tune the pruned models for 10 epochs. Although both normal accuracy and watermark accuracy drop after pruning, they are both recovered during the fine-tuning process. Figure 8 shows the normal classification accuracy and watermark accuracy after fine-pruning for different ratios of neurons pruned. We report the average with standard deviation of 5 different watermarked models. We can see that for all tasks, our watermark accuracy stay high with the normal classification accuracy.

9.3 Model Extraction Attack

Finally, we consider the possible use of model extraction attacks [21, 32] to bypass watermarks. In a model extraction attack, the attacker gathers unlabeled input data and uses the classification results of the target model to label the data. With this newly labeled data, it then trains a new watermark-free, substitute model that mimics the behavior of the original. Given our assumption that the attacker has unfettered access to the target model, model extraction attacks are extremely difficult to prevent.

We observe that extraction attacks provide limited value in the context of watermarked models. Recall that watermarks are designed to protect proprietary models, which are valuable because (a) it can be difficult to get large volume of data for a specific target domain, (b) it is time-consuming to label such datasets, and (c) it is computationally costly to train models given labeled data. Successful extraction attacks against watermarks do not solve challenges (a) or (c). Ex-

⁵The only publicly available ABS code is a binary operating on CIFAR-10. We contacted the authors and, after they declined to provide additional code, asked them to run their proprietary code on 2 GTSRB models. They could not detect our watermark.

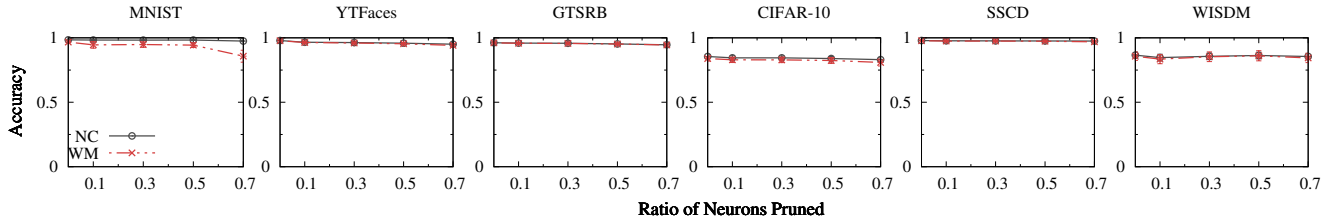


Figure 8: The impact of fine-pruning on the model’s normal classification (NC) and watermark classification accuracy (WM), as a function of the ratios of neurons pruned. We report average results of the performance with standard deviation over 5 different watermarked models for each task.

traction attacks solve (b), but likely through normal licensing from the model owner.

Here, we use some experimental results to better understand the practical challenges of solving (a): getting unlabeled training data in the application domain, and (c): training a model from extracted data.

In-distribution Data. For some tasks, collecting a large set of high-quality, task-specific data (even unlabeled) is still costly or impractical. In this case, attackers can choose to use alternative sources from other domains (*e.g.* online scraping or self generation). We experiment to see if out-of-distribution datasets can serve as unlabeled data in model extraction attacks, with 3 datasets: ImageNet, YouTube Faces, and randomly-generated images. We use each dataset to build a substitute model for the watermarked GTSRB model (traffic sign recognition) using model extraction via Papernot *et al.* [21] (results using the original Tramer attack [32] are included Table 18 in the appendix).

Table 8 lists the classification accuracy of the substitute models as a function of the training data volume. ImageNet performs the best among the three data sources, but just to achieve a model that has lower classification accuracy than the original (94.0% vs. 96.1%), it requires input training data that is 255% of the original in-distribution training dataset. Our tests were unable to train a model with accuracy equal to the original, due to high computational costs [21]. Achieving equal accuracy for the Tramer attack [32] required input data roughly equivalent to 1275% of the original training dataset.

Training and Extraction Costs. Next we consider the computational costs of training a model and the extraction attack itself. We perform the extraction attack based on [21] on GTSRB dataset, assuming the attacker has 5k training images. Compared to training a model from scratch with the entire training dataset, model extraction saves some training time ($12.80 \pm 6.72\%$ of the time required to train from scratch).

However, a realistic view of computation should also consider the costs of computing the query images used in model extraction. Our experiments show that using current methods [21], query image generation is actually much more computationally costly (in time) than model training itself. To obtain a model with similar accuracy as the original (95%), an end-to-end attack including extraction and model training takes roughly a factor of 9.52 ± 1.89 times longer than train-

ing from scratch with labeled data.

These results suggest that while powerful, extraction attacks provide limited benefit to attackers looking to obtain the target model compared to training the model itself.

Potential Defenses against Model Extraction. Finally, we note that there may be ways to limit the impact of model extraction attacks on watermarks. Recent work proposes watermarks that “entangles” with normal data through the use of *soft nearest neighbor loss* [13]. An attacker extracting a model with an *entangled watermark* inevitably extracts the watermark into their stolen model. As part of continuing work, we are actively investigating similar techniques to entangle null embeddings such that they are forcibly learned by extraction attacks.

10 Discussion and Conclusion

We propose a new ownership watermark system for DNN models, which achieves the critical property of piracy resistance that has been missing from all existing watermark designs. Core to our watermark design is *null embedding*, a new training method that creates a strong dependency between normal classification accuracy and a given watermark when a model is initially trained. Null embeddings constrain the classification space, and cannot be replaced or added without breaking normal classification.

Limitations remain in our proposed system. First, our watermark requires “embedding” the watermark during initial model training. This leads to some (perhaps unavoidable) inconveniences. Since a watermark cannot be repeated or removed, a model owner must choose the watermark before training a model, and any updates to the watermark requires retraining the model from scratch. Similarly, our watermark cannot be directly added to already-trained models – the owner needs to retrain the model from scratch. Second, our experimental validation has been limited by computational resources. We could not test our watermark on the largest models, *e.g.* ImageNet as a result. Our smaller models and their image sizes limited the size of watermarks in our tests ($6 \times 6 = 36$ pixels). In practice, ImageNet’s larger input size means it would support proportionally larger watermarks ($24 \times 24 = 576$ pixels). We are building a much larger GPU cluster to enable larger scale watermark experiments.

In ongoing work, we are exploring how null embedding

might be extended to other domains like audio or text. Finally, we continue to test and evaluate our watermark implementation, with the goal of releasing a full implementation to the research community in the near future.

References

- [1] ADI, Y., BAUM, C., CISSE, M., PINKAS, B., AND KESHET, J. Turning your weakness into a strength: Watermarking deep neural networks by backdooring. In *Proc. of USENIX Security* (2018).
- [2] ADIWARDANA, D., LUONG, M.-T., SO, D. R., HALL, J., FIEDEL, N., ET AL. Towards a human-like open-domain chatbot. *arXiv preprint arXiv:2001.09977* (2020).
- [3] BENDER, W., GRUHL, D., MORIMOTO, N., AND LU, A. Techniques for data hiding. *IBM Systems Journal* (1996).
- [4] BUCHNER, J. Synthetic speech commands: A public dataset for single-word speech recognition.
- [5] CHEN, H., ROUHANI, B. D., FU, C., ZHAO, J., AND KOUSHANFAR, F. Deepmarks: A secure fingerprinting framework for digital rights management of deep learning models. In *Proc. of ICMR* (2019).
- [6] DARVISH ROUHANI, B., CHEN, H., AND KOUSHANFAR, F. Deepsigns: An end-to-end watermarking framework for ownership protection of deep neural networks. In *Proc. of ASP-LOS* (2019).
- [7] EYKHOLT, K., ET AL. Robust physical-world attacks on deep learning models. *arXiv preprint arXiv:1707.08945* (2017).
- [8] FAN, L., NG, K. W., AND CHAN, C. S. Rethinking deep neural network ownership verification: Embedding passports to defeat ambiguity attacks. *arXiv preprint arXiv:1909.07830* (2019).
- [9] FREDRIKSON, M., JHA, S., AND RISTENPART, T. Model inversion attacks that exploit confidence information and basic countermeasures. In *Proc. of CCS* (2015).
- [10] HAN, S., MAO, H., AND DALLY, W. J. Deep compression: Compressing deep neural networks with pruning, trained quantization and huffman coding. In *Proc. of ICLR* (2016).
- [11] HAN, S., POOL, J., TRAN, J., AND DALLY, W. Learning both weights and connections for efficient neural network. In *Proc. of NeurIPS* (2015).
- [12] HARTUNG, F., AND KUTTER, M. Multimedia watermarking techniques. *Proc. of the IEEE* 87, 7 (1999).
- [13] JIA, H., CHOQUETTE-CHOO, C. A., AND PAPERNOT, N. Entangled watermarks as a defense against model extraction. *arXiv preprint arXiv:2002.12200* (2020).
- [14] KRIZHEVSKY, A., ET AL. Learning multiple layers of features from tiny images. Master’s thesis, UToronto, 2009.
- [15] KUTTER, M., JORDAN, F. D., AND BOSSEN, F. Digital signature of color images using amplitude modulation. In *Proc. of Electronic Imaging* (1997).
- [16] KWAPISZ, J. R., WEISS, G. M., AND MOORE, S. A. Activity recognition using cell phone accelerometers. *ACM SigKDD Explorations* 12, 2 (2011).
- [17] LECUN, Y., BOTTOU, L., BENGIO, Y., HAFFNER, P., ET AL. Gradient-based learning applied to document recognition. *Proc. of the IEEE* 86, 11 (1998).
- [18] LIU, K., DOLAN-GAVITT, B., AND GARG, S. Fine-pruning: Defending against backdooring attacks on deep neural networks. In *Proc. of RAID* (2018).
- [19] LIU, Y., ET AL. Abs: Scanning neural networks for backdoors by artificial brain stimulation. In *Proc. of CCS* (2019).
- [20] MOGELMOSE, A., TRIVEDI, M. M., AND MOESLUND, T. B. Vision-based traffic sign detection and analysis for intelligent driver assistance systems: Perspectives and survey. *Proc. of T-ITS* (2012).
- [21] PAPERNOT, N., ET AL. Practical black-box attacks against machine learning. In *Proc. of ASIACCS* (2017).
- [22] PARKHI, O. M., VEDALDI, A., ZISSERMAN, A., ET AL. Deep face recognition. In *BVMC* (2015), vol. 1.
- [23] RIBEIRO, M., GROLINGER, K., AND CAPRETZ, M. A. M. Mlaas: Machine learning as a service. In *Proc. of ICMLA* (2015).
- [24] SCHROFF, F., KALENICHENKO, D., AND PHILBIN, J. Facenet: A unified embedding for face recognition and clustering. In *Proc. of CVPR* (2015).
- [25] STALLKAMP, J., SCHLIPSING, M., SALMEN, J., AND IGEL, C. Man vs. computer: Benchmarking machine learning algorithms for traffic sign recognition. *Neural Networks* (2012).
- [26] SUN, Y., WANG, X., AND TANG, X. Deep learning face representation from predicting 10,000 classes. In *Proc. of CVPR* (2014).
- [27] SWANSON, M. D., ZHU, B., AND TEWFIK, A. H. Multiresolution scene-based video watermarking using perceptual models. *Proc. of IEEE JSAC* (1998).
- [28] SWANSON, M. D., ZHU, B., TEWFIK, A. H., AND BONEY, L. Robust audio watermarking using perceptual masking. *Signal Processing* 66, 3 (1998).
- [29] SZYLLER, S., ATLI, B. G., MARCHAL, S., AND ASOKAN, N. Dawn: Dynamic adversarial watermarking of neural networks. *arXiv preprint arXiv:1906.00830* (2019).
- [30] TANAKA, K., NAKAMURA, Y., AND MATSUI, K. Embedding secret information into a dithered multi-level image. In *Proc. of IEEE Milcom* (1990).
- [31] TILKI, J. F., AND BEEX, A. A. Encoding a hidden digital signature onto an audio signal using psychoacoustic masking. In *Proc. of ICSPAT* (1996).
- [32] TRAMÈR, F., ZHANG, F., JUELS, A., REITER, M. K., AND RISTENPART, T. Stealing machine learning models via prediction apis. In *Proc. of USENIX Security* (2016).
- [33] UCHIDA, Y., NAGAI, Y., SAKAZAWA, S., AND SATOH, S. Embedding watermarks into deep neural networks. In *Proc. of ICMR* (2017).
- [34] VAN SCHYNDEL, R. G., TIRKEL, A. Z., AND OSBORNE, C. F. A digital watermark. In *Proc. of ICIP* (1994).
- [35] WANG, B., ET AL. Neural cleanse: Identifying and mitigating backdoor attacks in neural networks. In *Proc. of S&P* (2019).

Layer Name	Layer Type	# of Channels	Filter Size	Activation	Connected to
conv_1	Conv	32	5×5	ReLU	
pool_1	MaxPool	32	2×2	-	conv_1
conv_2	Conv	64	5×5	ReLU	pool_1
pool_2	MaxPool	64	2×2	-	conv_2
fc_1	FC	512	-	ReLU	pool_2
fc_2	FC	10	-	Softmax	fc_1

Table 9: Model Architecture for MNIST.

Layer Name	Layer Type	# of Channels	Filter Size	Activation	Connected to
conv_1	Conv	20	4×4	ReLU	
pool_1	MaxPool	20	2×2	-	conv_1
conv_2	Conv	40	3×3	ReLU	pool_1
pool_2	MaxPool	40	2×2	-	conv_2
conv_3	Conv	60	3×3	ReLU	pool_2
pool_3	MaxPool	60	2×2	-	conv_3
fc_1	FC	160	-	-	pool_3
conv_4	Conv	80	2×2	ReLU	pool_3
fc_2	FC	160	-	-	conv_4
add_1	ADD	-	-	ReLU	fc_1, fc_2
fc_3	FC	1283	-	Softmax	add_1

Table 10: Model Architecture for YTFaces.

Layer Name	Layer Type	# of Channels	Filter Size	Activation	Connected to
conv_1	Conv	32	3×3	ReLU	
conv_2	Conv	32	3×3	ReLU	conv_1
pool_1	MaxPool	32	2×2	-	conv_2
conv_3	Conv	64	3×3	ReLU	pool_1
conv_4	Conv	64	3×3	ReLU	conv_3
pool_2	MaxPool	64	2×2	-	conv_4
conv_5	Conv	128	3×3	ReLU	pool_2
conv_6	Conv	128	3×3	ReLU	conv_5
pool_3	MaxPool	128	2×2	-	conv_6
fc_1	FC	512	-	ReLU	pool_3
fc_2	FC	512	-	ReLU	fc_1
fc_3	FC	43	-	Softmax	fc_2

Table 11: Model Architecture for GTSRB.

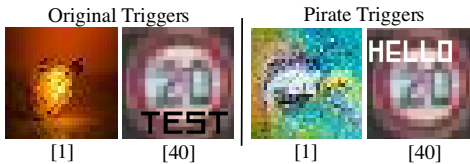


Figure 9: Examples of original and pirate triggers used to recreate [1] and [41].

- [36] WANG, B., AND GONG, N. Z. Stealing hyperparameters in machine learning. In *Proc. of S&P* (2018).
- [37] WANG, T., AND KERSCHBAUM, F. Attacks on digital watermarks for deep neural networks. In *Proc. of ICASSP* (2019).
- [38] WOLFGANG, R. B., PODILCHUK, C. I., AND DELP, E. J. Perceptual watermarks for digital images and video. *Proc. of the IEEE* 87, 7 (1999).
- [39] YANG, Z., DANG, H., AND CHANG, E.-C. Effectiveness of distillation attack and countermeasure on neural network watermarking. *arXiv preprint arXiv:1906.06046* (2019).
- [40] YAO, Y., ET AL. Complexity vs. performance: empirical analysis of machine learning as a service. In *Proc. of IMC* (2017).
- [41] ZHANG, J., ET AL. Protecting intellectual property of deep neural networks with watermarking. In *Proc. of ASIACCS* (2018).

A Additional Experimental Materials

This section contains additional information that supplements technical details presented in the main text.

Layer Name	Layer Type	# of Channels	Filter Size	Activation	Connected to
conv_1	Conv	32	3×3	ReLU	
conv_2	Conv	32	3×3	ReLU	conv_1
pool_1	MaxPool	32	2×2	-	conv_2
conv_3	Conv	64	3×3	ReLU	pool_1
conv_4	Conv	64	3×3	ReLU	conv_3
pool_2	MaxPool	64	2×2	-	conv_4
conv_5	Conv	128	3×3	ReLU	pool_2
conv_6	Conv	128	3×3	ReLU	conv_5
pool_3	MaxPool	128	2×2	-	conv_6
fc_1	FC	512	-	ReLU	pool_3
fc_2	FC	512	-	ReLU	fc_1
fc_3	FC	43	-	Softmax	fc_2

Table 12: Model Architecture for CIFAR-10.

Layer Name	Layer Type	# of Channels	Filter Size	Activation	Connected to
conv_1	Conv	32	5×5	ReLU	
pool_1	MaxPool	32	2×2	-	conv_1
conv_2	Conv	64	3×3	ReLU	pool_1
pool_2	MaxPool	64	2×2	-	conv_2
fc_1	FC	512	-	ReLU	pool_2
fc_2	FC	10	-	Softmax	fc_1

Table 13: Model Architecture for SSCD.

Layer Name	Layer Type	# of Channels	Filter Size	Activation	Connected to
conv_1	Conv	120	5	ReLU	
conv_2	Conv	120	5	ReLU	conv_1
pool_1	MaxPool	120	3	-	conv_2
conv_3	Conv	180	5	ReLU	pool_1
conv_4	Conv	180	5	ReLU	conv_3
pool_2	MaxPool	180	3	-	conv_4
fc_1	FC	512	-	ReLU	pool_2
fc_2	FC	512	-	ReLU	fc_1
fc_3	FC	6	-	Softmax	fc_2

Table 14: Model Architecture for WISDM.



Figure 10: Additional triggers used to successfully conduct a watermark piracy attack against [41].

Model architecture & training configuration. Tables 9, 11, 10, 12, 13, and 14 list the architectures of the different models used in our experiments. For all six tasks, we use convolutional network networks. We vary the number of layers, channels, and filter sizes in the models to accommodate different tasks. Table 16 describes the details of the training configurations used for each task.

Description of §4's experiments on existing watermark designs. We provide additional details on our experiments in §4, which study the performance of two existing watermark designs ([1] and [41]) under piracy attacks. We describe the watermark triggers and model training configurations used in our experiments.

Watermark Triggers. For [1], the original trigger set we use is the same as the trigger set used in [1]. To collect the pirate trigger set, we randomly choose 100 images of abstract art from Google Images, resize them to fit our model, and assign labels for each of them. Note that both the original and pirate trigger sets contain exactly 100 images. For [41], we use a trigger very similar to one used in their paper – the word "TEXT" written in black pixels at the bottom of an im-

Task	Before Piracy							After Piracy						
	NC (%)	Owner WM			Pirate WM (%)			NC (%)	Owner WM			Pirate WM (%)		
		true (%)	null (%)	WM (%)	true (%)	null (%)	WM (%)		true (%)	null (%)	WM (%)	true (%)	null (%)	WM (%)
MNIST	98.4 ± 0.2	96.8 ± 1.2	100.0 ± 0.0	96.8 ± 1.2	10.2 ± 0.9	6.9 ± 25.2	0.7 ± 2.5	21.2 ± 27.3	12.9 ± 11.4	16.0 ± 36.6	2.8 ± 9.0	20.5 ± 26.0	16.0 ± 42.5	11.9 ± 27.6
YTFaces	97.8 ± 0.5	97.7 ± 0.5	100.0 ± 0.0	97.7 ± 0.5	1.3 ± 8.8	0.0 ± 0.0	0.0 ± 0.0	19.0 ± 22.7	3.0 ± 14.6	59.1 ± 48.2	1.6 ± 10.9	5.2 ± 17.9	59.1 ± 45.7	5.2 ± 17.9
GTSRB	96.1 ± 0.5	95.9 ± 0.9	100.0 ± 0.0	95.9 ± 0.9	6.7 ± 15.8	3.1 ± 17.0	0.2 ± 0.8	11.2 ± 28.0	9.5 ± 25.4	16.0 ± 36.7	6.8 ± 24.1	11.1 ± 27.7	16.0 ± 27.3	7.0 ± 24.0
CIFAR-10	85.6 ± 1.2	84.1 ± 1.6	100.0 ± 0.0	84.1 ± 1.6	10.1 ± 0.4	11.0 ± 31.3	1.1 ± 3.2	24.4 ± 26.9	21.3 ± 23.9	17.1 ± 37.5	6.8 ± 20.1	22.5 ± 24.7	17.1 ± 45.4	13.5 ± 25.5
SSCD	97.9 ± 0.2	97.7 ± 0.4	100.0 ± 0.0	97.7 ± 0.4	10.3 ± 1.9	9.0 ± 28.6	0.9 ± 2.9	34.5 ± 35.1	20.6 ± 24.9	23.9 ± 42.5	10.3 ± 25.4	34.1 ± 34.8	23.9 ± 47.5	27.8 ± 38.9
WISDM	87.7 ± 2.4	87.2 ± 2.9	100.0 ± 0.0	87.2 ± 2.9	29.7 ± 5.1	17.9 ± 38.1	5.6 ± 11.9	35.5 ± 31.1	25.3 ± 22.6	33.5 ± 46.8	12.2 ± 23.3	33.7 ± 29.6	33.5 ± 49.7	25.2 ± 33.8

Table 15: Normal classification and watermark accuracy before and after an adversary tries to embed a pirate watermark into the model. “null” and “true” refer to classification accuracy for null and true embedding, and “WM” represents overall watermark classification accuracy. Each piracy result is averaged over 500 pirate watermarks and 10 watermarked models.

Tasks	Training Configuration
MNIST	lr=0.001, decay=0, opt=sgd, bsize=128, max_e=300, ir=0.5
YTFaces	lr=0.001, decay=1e-6, opt=adam, bsize=128, max_e=10, ir=0.5
GTSRB	lr=0.02, decay=2e-5, opt=sgd, bsize=128, max_e=120, ir=0.1
CIFAR-10	lr=0.02, decay=2e-5, opt=sgd, bsize=128, max_e=1000, ir=0.1
SSCD	lr=0.001, decay=1e-6, opt=sgd, bsize=32, max_e=500, ir=0.1
WISDM	lr=0.005, decay=2e-5, opt=sgd, bsize=32, max_e=300, ir=0.1

Table 16: Hyper-parameters for model training for all six tasks. lr represents learning rate, opt represents optimizer, bsize represents batch_size, max_e represents maximum of epochs given, and ir represents inject_ratio.

Task	[1]		[41]	
	Inject Ratio	Piracy Epochs	Inject Ratio	Piracy Epochs
MNIST	18.8%	10	10%	10
GTSRB	6.2%	10	10%	10
YTFaces	6.2%	1	10%	1
CIFAR-10	6.2%	10	25%	10

Table 17: Learning parameters for piracy attacks on prior watermarking schemes.

age. The pirate trigger is the word “HELLO” written in white pixels at the top. Figure 9 shows triggers used for [41], and one sample from both original and pirate trigger sets [1].

For completeness, we tried several triggers for the piracy attack on [41] and found that all are successful (> 95% pirate trigger accuracy). These are shown in Figure 10.

Training Configurations. To train the original watermarked models for both methods, we use the training configurations shown in Table 16 and the watermark injection ratios in Table 17. For all tasks, we assume the attacker only has 5k training data for MNIST, YTFaces, GTSRB, and CIFAR-10. The same configuration is used for the piracy experiments on our own watermarking system.

Additional results for §7.3. Table 15 provides the detailed numerical results on Figure 4(a)-(b), in terms of normal classification accuracy (NC), owner’s watermark classification accuracy and pirate watermark classification accuracy. For the latter two, we also provide the individual accuracy of null and true embeddings.

Experimental setup for transfer learning in §8. The dataset for the student task is LISA (3,987 training images and 340 testing images of 17 US traffic signs). We resize all the images to (48, 48, 3) to allow transfer learning. During transfer learning, we fine tune the student model for 200

Data	50k	100k	376k	500k
ImageNet	89.7 ± 4.2%	92.9 ± 2.1%	93.9 ± 1.8	94.1 ± 1.3%
YouTube Faces	65.4 ± 5.2%	74.6 ± 2.1%	78.0 ± 3.6	-
Random	5.0 ± 0.6%	5.2 ± 0.4%	5.02 ± 0.4	5.2 ± 0.8%

Table 18: Normal classification accuracy of the substitute model built by model extraction [32] using each of the three data sources. For each entry in the first row, we show # of (unlabeled) images used to train the substitute model. YTFaces only has 376k training data, so we cannot run the 500k result. The size of original model training data is 39k.

epochs using student training data, using SGD optimizer with 0.01 learning rate and 0 decay.

Additional details on countermeasures in §9. We list the detailed configurations and discussion for countermeasures.

Model Extraction Attack. To launch an attack on GTSRB, we create a substitute model with the same model architecture in Table 11. To train the substitute model from scratch we use the same training configurations for GTSRB in Table 16 but do not add watermarks to any training data. We include the In-distribution data requirements for [32] in Table 18. Even with 12.75x input data from ImageNet, the normal classification accuracy for substitute models is still lower than that of the original model (94.1% vs. 96.1%).

Model Distillation Attack [39]. Distillation is similar to the model extraction attack, but it introduces temperatures when using the target model to label the data. Prior work suggests that model distillation can train accurate models using smaller datasets (compared to datasets used to train models from scratch). However, we believe this conclusion was due in large part to unnecessarily large training datasets used to train models from scratch.

We performed detailed experiments, (on GTSRB), where we varied parameters (different temperatures) to find the optimal (smallest) training subset that would produce (via distillation) a model with accuracy within 3% of the ideal model. The result was a small training sample (12.8% of the original) that produced accuracy of 95.4%. Our tests show that the same exact dataset, when used to train GTSRB models from scratch, produces a model with 95.0% accuracy. We also validated this on MNIST and CIFAR-10, where the distilled dataset, when used to train a model from scratch, produced a model with accuracy matching that of the distilled model.